Averaged Small Signal Model of aPush-Pull Converter with Parasitic Elements in Continuous Mode

Atila Skandarnezhad[1*], Noruz Abdollahi[2]

Abstract–This paper presents the small-signal modeling of amodifiedpush-pull converter using averaged circuit method.Parasitic elements are considered to increase the accuracy of the proposed technique. In the design process of converters it is desirable to assess as many critical design parameters and parasitic effects by simulation as possible, since the control is hard to tune after fabrication.The low frequency small-signal model is doneusing state space averaging technique and two main power-stage transfer functions are derived, which are control-to-output voltage transfer function and input-to-output voltage transfer function.Using the proposed model of the converter we can analyze and simulate the time domain transient behavior of the system accurately and intuitively. The resulting model is a time averaged equivalent circuit model where all branch currents and node voltages correspond to their averaged values of the corresponding original currents and voltages.The model is applicable to bothcurrent and voltage mode control. The model has the principleadvantage that it is simple to derive and it takes the same form asthe switching converter that it is derived from. In the model,the MOSFET switches are replaced by dependent current andvoltage sources equal to the average current through theswitch, or average voltage across the switch.The validity of the proposed model was verified by simulation and experimental results for a specified design example. The method of modelling presented here helps to design the inverter effectively and better choosing the controller component values.

Keywords:Push-pullconverter, Small signal model, Averaging Technique,Continuous mode

1. Introduction

By their very nature, switching power supplies are timevariant and non-linear. As a result, conventional linear controltechniques cannot be directly applied to analyze converterdynamics. However, to design an appropriate feedback systemthat can assure stability and good dynamic performance, weneed a dynamic model of the switching converter. Thedynamic model should model the dominant low frequencybehavior of the system, but should neglect behavior at andbeyond the switching frequency [1-3].

The push-pull converter is a DC/DC converter that uses a transformer to increase or decrease the output voltage depending on the transformer ratio and provide galvanic isolation for the load [4]. With multiple output windings, it is possible to provide both higher and lower voltage outputs simultaneously where used in ATX power supplies

widely.While it looks superficially like a flyback converter, it operates in a fundamentally different way, and is generally more energy efficient. Flyback converter stores energy in the magnetic field in the transformer air gap during the time the converter switching element (transistor) is conducting. When the switch turns off, the stored magnetic field collapses and the energy is transferred to the output of the flyback converter as electric current. The flyback converter can be viewed as two inductors sharing a common core with opposite polarity windings [5,6].

In contrast, the push-pull converter which is based on a transformer with samepolarity windings, higher magnetic inductance, and no air gap does not store energy during the conduction time of the switching element transformers cannot store a significant amount of energy, unlike inductors.Instead, energy is passed directly to the output of the push-pull converter by transformer action during the switch conduction phase [7,8].

Many small signal models have been developed forswitching converters, however, these models can only predictsmall signal stability in the vicinity of their operating point, butconverters can become unstable when they experience a largeperturbation, such as large transient load changes which arecommon for traditional systems [9].

1* **CorrespondingAuthor:**Department of Electrical Engineering, Aliabad Katoul Branch, Islamic Azad University, AliabadKatoul, Iran.

Email:eskandarnejad@aliabadiau.ac.ir

2Department of Electrical Engineering, Aliabad KatoulBranch, Islamic Azad University, Aliabad Katoul, Iran. Email:abdollahi@aliabadiau.ac.ir

The proposed modified PWM dc–dc converter contains two transistors, a transformer, and a rectifier. Its main advantage is that the voltage stresses of the transistors are low and equal to the maximum dc input voltage of the converter. It can handle the rectified dc voltage of the European 220Vrms + 10% utility single-phase line, which is usually in the range from 280 to 340 V. Power transistors with a voltage rating of 400 to 500V are readily available and may be used in this converter; therefore, the converter is used in off-line power supplies. Another advantage is that the core saturation problems are minimized because the dc component of the current through the primary is zero due to the coupling or blocking capacitors in series with the primary [10]. Since the primary is driven in both directions, the core is utilized more effectively. The disadvantages are the requirement of an additional power transistor and of an isolated driver for the upper transistor. Typically, the converter is suitable for mediumpower applications from 100W to 1kW and is widely used in telecommunications power supplies. It belongs to the buck family converter [11].

The averaging method is based on analytical averaging of switch circuit equations describing linear equivalent circuits for different states of a converter determined by the on–off status of the transistor and the diode. The averaged equations are weighed according to the fraction of the switching cycle, during which the converter remains in a given state. However, the state-space averaging method requires considerable matrix algebra manipulation and is sometimes tedious, especially when the converter circuit contains a large number of elements or parasitic components [12]. Moreover, it provides little insight into the converter behavior. On the other hand, in many power electronic circuits, the average values of voltages and currents are of interest, rather than their instantaneous values. The circuit-averaging method leads to linear circuit models. These models are relatively simple, provide good intuitive insight into converter behavior, can be used for deriving various transfer functions and step responses, and are compatible with general purpose electronic circuit simulators. In addition, control loops for PWM converters can be designed by applying linear control techniques [13].

There are some advantages to the proposed model such: it is simple sincethey averaged circuit model has the same topology as the switching converter. It is general sincethe model can be applied to all isolated and non-isolated DC converters under current, or voltage mode control [14]. It is powerful sincethe effects of slope compensation andparasitic elements and filtering can be easily included. It is unified sincethe small signal transfer functions and input-output relations can be derived from the large signal model.

2. The Converter Structure

The converter structure is depicted in Figure 1.
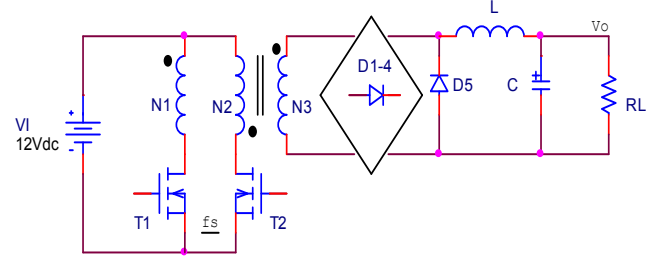
Fig. 1. The converter structure

By circuit analysis of the above converter in the lossless condition one can deduce the DC transfer function of voltage that is presented in (1) [3].

$$M_V = V_O/V_I = I_I/I_O = D/n \qquad (1)$$

Where V_O and I_O is the output voltage and current, V_I and I_I is the input voltage and current, D is duty cycle of transistor gate signal and n is the turn ratio of switching transformer: $n=N_3/N_1$ or $n=N_3/N_2$.

It is mentionable that, D value is between 0 - 0.5 since T_1 and T_2 are complementary. Figure 2, shows the boundary between current continuous conduction mode (CCM) and discontinuous conduction mode (CCM) of inductor current.
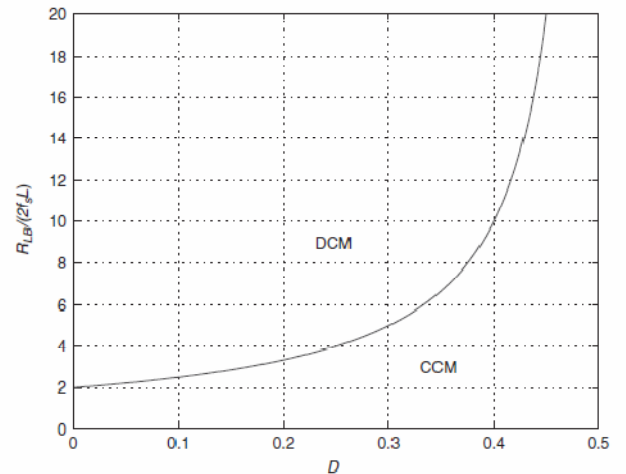
Fig. 2. Boundary between CCM and DCM.

In Figure 2, R_{LB} is the load resistor, $F_s$is the transistors switching frequency, L is the inductance. In Figure 1, two primary windings of the converter transformer have same and opposite direction. Then by little circuit manipulation can change it to the circuit depicted in Fig. 3.Since T_1 and T_2 switch in the complementary manner, the circuit simplifies by eliminating one of them and doubling the F_s.
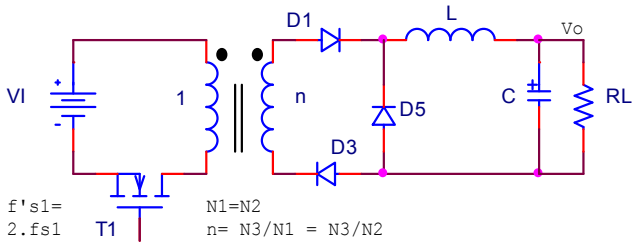
Fig. 3. Simplified form of the converter

3. Averaged switch network model

The state space technique offers an interesting but some complicated way for deriving small signal models of power converters. The difficulty is mainly due to the fact that this method is carried over the entire converter, manipulating numerous state variables that can easily be omitted or lost during the derivation process. Fortunately, averaged switch network technique exists that really simplifies the converter small signal studies. In the average circuit model, the average low frequency voltages across the model terminals and the average low frequency currents into its terminals are identical to those of the original switching network. The waveforms of the average current and voltage do not contain high frequency components. The high frequency components can be regarded as carriers. The average model is nonlinear and may be supposed linear for small ac signals. The linear part of a converter does not require averaging and linearization. This modeling strategy of PWM converters is similar to the transistor modeling and is based on two principles [15]:

(i) Replacement of the switching networkby an analog continuous circuit model.

(ii) Leaving the analog part composed of linear components unchanged.

Figure 4, Shows the single-ended transformer-less two switch network of the studied converter.
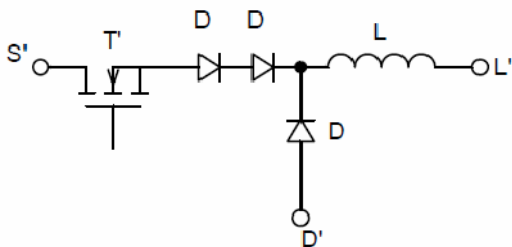
Fig. 4. Switching network.

The ideal part of the switching network is depicted in Fig. 5, which the MOSFET switch comes from primary side of the transformer and its r_{ds} resistor mirrored by n^2 factor [16].
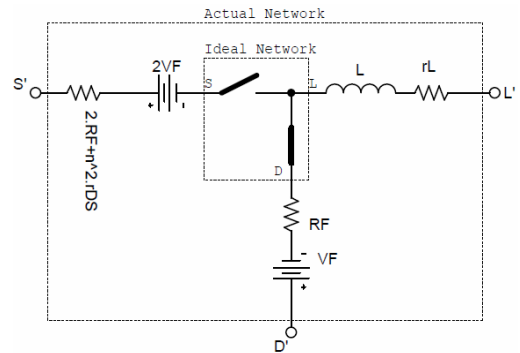
Fig. 5. Equivalent of the switching network

Symbols S' ,D' and L' are the switch, diode, inductor nodes of actual network respectively, and similarly apply to the ideal network too. The reflection rules can be applied to move the parasitic components from one branch to another with considering the energy conservation rule. Figure6, depicts the simplified averaged dc model of the actual network with the averaged resistances go to right branch.
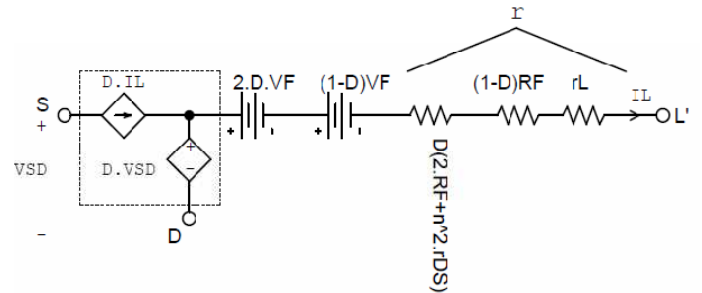
Fig. 6. Simplified network with parasitic part

Consider the operation of a PWM converter under external low frequency excitation also called low frequency perturbation, superimposed on the dc component. Each of the waveforms in a PWM converter under low frequency excitation contains three components:a dc component, a low frequency component of the frequency $f = \omega/(2\pi)$ and its harmonics, a high frequency component of the switching frequency fs and its harmonics. Only the dc and the low frequency components are of interest when studying control aspects of PWM converters. This is because the control signals of the closed loop PWM converters consist of dc and low frequency components.
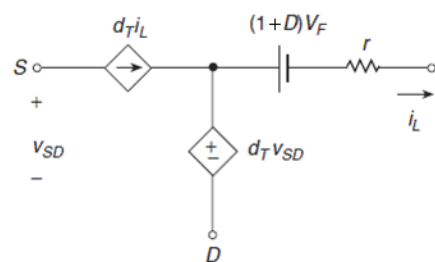
Fig. 7. Large signal model of switch network

Consequently, the low frequency components are used to characterize the dynamics of PWM systems. The large signal model of this network is in Figure 7. Where r is the sum of the mirrored resistors, where is stated in Eq. (2). r_{DS} ,R_F and r_L are the resistors of transistor, diode and inductor respectively and n is the transformer turns ratio.

$$r = D.n^2 r_{DS} + (1+D)R_F + r_L \quad (2)$$

Linearization of the large signal averaged model at a given operating point can be performed by expanding the equations to Taylor's series and neglecting the higher order terms. Linear small signal model can be obtained by assuming the perturbations that are expressed in (3)and(4).

$$d_T.i_L = (D+d)(I_L + i_l) = DI_L + Di_l + dI_L + \cancel{di_l}^{\,0} (3)$$

$$d_T.v_{SD} = (D+d)(V_{SD} + v_{sd}) = DV_{SD} + Dv_{sd} + dV_{SD} + \cancel{dv_{sd}}^{\,0} (4)$$

By neglecting the products of small signal components, di_l and $dv_s$where equations (3) and(4) can be represented by a circuit model of the actual switching network shown in Figure8. The equation contains both dc and ac small signal components, depicted as dependent sources. According to Shannon's sampling theorem this dynamic model is valid up to the double of switching frequency or $f'_{s1} = 2f_{s1}$.
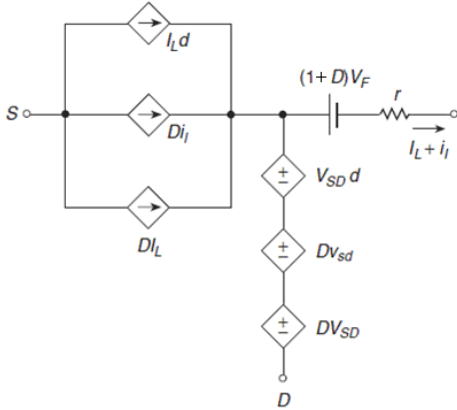
Fig. 8. Averaged dc and small signal model

Since circuit averaging involves averaging and small-signal linearization, it is equivalent to the state-space averaging. However, in many cases circuit averaging is easier to apply, and allows the small-signal ac model to be written almost by inspection. The circuit averaging technique can also be applied directly to a number of different types of converters and switch elements, including phase-controlled rectifiers, PWM converters operated in discontinuous mode or current programmingconverters.

4. Replacing the Simplified Switch Network

By replacing switching devices in the buck converter that is shown in Figure 9, with the averaged model in Figure8, can derive the dc and small signal transfer functions of audio success-ability and control-to-output. To study the dynamic behavior of the inverter, Responses of the output voltage to step change in input voltage and D are shown.
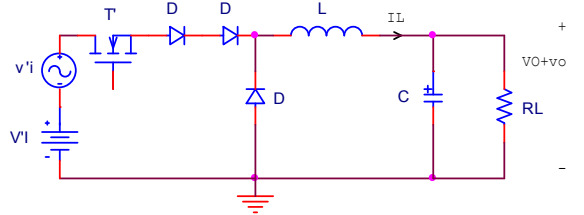
Fig. 9. Final buck converter

DC model can be derived by setting to zero the ac source in Figure8, which is depicted in Figure 10.
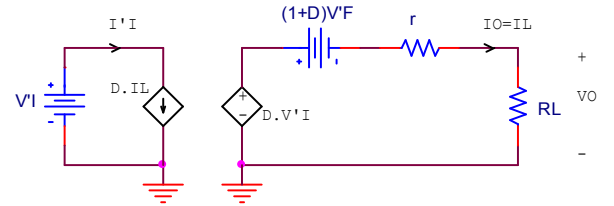
Fig. 10.DC model of the converter

Using Kirchhoff voltage law and according to Eq. (5),(6)

$$DV'_I - (1+D)V_F - rI_L - R'_L I_L = 0 \quad (5)$$

$$V'_O = R'_L I_L \quad , \quad V'_I = n.V_I \quad (6)$$

Which yields the dc input-to-output and control-to-output voltage transfer functions as inEq. (7) ,(8).

$$H_{V'_O - V'_I}(D) = \frac{V'_O}{V'_I} = D\frac{R'_L}{R'_L + r}(1-(\frac{1}{D}+1)\frac{V_F}{V'_I}) \quad (7)$$

$$H_{V'_O - D}(D) = \frac{V'_O}{D} = V'_I \frac{R'_L}{R'_L + r}(1-(\frac{1}{D}+1)\frac{V_F}{V'_I}) \quad (8)$$

And similarly Eq. (9)-(11) determinesthe dc input-to-output current ratio and efficiency.

$$I'_I = D.I_L \qquad , \qquad I'_O = I_L \quad (9)$$

$$H_{I'_O - I'_I}(D) = \frac{I'_O}{I'_I} = \frac{1}{D} \quad (10)$$

$$\eta = \frac{P_O}{P_I} = \frac{V_O I_O}{V_I I_I} = \frac{V'_O I'_O}{V'_I I'_I} = (H_{V'_O - V'_I})(H_{I'_O - I'_I}) \quad (11)$$

Now, small signal model can be derived by setting to zero the dc source in Figure 8, where is depicted in Figure 11. Note the current source is soldered to ground node and parallelvoltage-current source is replaced by voltage type.
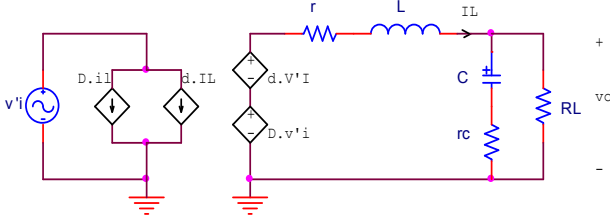
Fig. 11. Small signal model of the converter

By considering Eq. (13), small signal audio success-ability or input-to-output voltage transfer function could be deduced by eliminating the dv'$_i$ in Figure 11, where is stated in Eq. (12) and (14) consequently.

$$Z_1 = r + SL \quad , \quad Z_2 = R'_L \| (r_C + \frac{1}{SC}) \quad (12)$$

$$v'_o = D.v'_i \frac{Z_2}{Z_1 + Z_2} \qquad (13)$$

$$h_{v_o - v_i}(s) = K_1 \frac{1 + \frac{s}{\omega_z}}{1 + \frac{s}{Q\omega_o} + (\frac{s}{\omega_o})^2} \qquad (14)$$

Quality factor and natural frequency stated in (15) - (18).

$$K_1 = D \frac{R'_L}{R'_L + r} \qquad (15)$$

$$\omega_z = \frac{1}{r_C.C} \qquad (16)$$

$$Q = \frac{\sqrt{LC(R'_L + r)(R'_L + r_C)}}{L + CR'_L(r + r_C)} \qquad (17)$$

$$\omega_o = \sqrt{\frac{R'_L + r}{LC(R'_L + r_C)}} = \frac{1}{\sqrt{\tau_C.\tau_L}} \qquad (18)$$

Capacitor and inductor time constants are stated in (19).

$$\tau_C = C(R'_L + r_C) \quad , \quad \tau_L = \frac{L}{(R'_L + r)} \quad (19)$$

Similarly, can determine the small signal control-to-output (or duty cycle-to-output) voltage transfer function by setting to zero the Dv'$_i$ source in Fig. 11, by(20) – (22).Fortunately, control-to-output transfer function has not right half plane zero that is seen in boost and buck-boost types. Damping ratio can be determined using: $\xi = 1/(2Q)$.

$$v'_o = D.v'_i \frac{Z_2}{Z_1 + Z_2} \qquad (20)$$

$$h_{v_o - d}(s) = K_2 \frac{1 + \frac{s}{\omega_z}}{1 + \frac{s}{Q\omega_o} + (\frac{s}{\omega_o})^2} \qquad (21)$$

$$K_2 = V'_I \frac{R'_L}{R'_L + r} \qquad (22)$$

The delay t_d introduced by a power transistors driver and pulse width modulator on the duty cycle can be described by a function stated and approximated by Eq. (23).

$$h_{delay}(s) = e^{-st_d} \approx \frac{s - \frac{2}{t_d}}{s + \frac{2}{t_d}} \qquad (23)$$

Then the delayed control-to-output transfer function will be stated by the following equation.

$$h_{v_o - d}(s) = K_2 \frac{1 + \frac{s}{\omega_z}}{1 + \frac{s}{Q\omega_o} + (\frac{s}{\omega_o})^2} \times \frac{s - \frac{2}{t_d}}{s + \frac{2}{t_d}} \quad (24)$$

5. Simulation and Experimental Results

Figure 12; indicate this paper experimental test hardware.Experimental data can be reproduced by using a variety of different investigators and mathematical analysis may be performed on these data.

Fig. 12. Experimental tested converter.

The transformer's secondary voltage is rectified and filtered suitably to get the desired quality ofoutput voltage waveform. The filter inductor and capacitor values need to be chosen optimally toarrive at a cost-effective, less bulky power supply,converter components value is seen below.

Table 1. Component values

Symbol	Description	Value
V_F	Diode threshold voltage	0.6V
R_F	Diode forward resistor	0.075Ω
r_{DS}	MOSFET on-resistance	0.02 Ω
L	Inductor value	40uH
r_L	ESR* of inductor	0.08 Ω
C	Capacitor value	68uF
r_C	ESR of capacitor	0.11Ω
n	transformer turn ratio	40
f_{S1}	Switching frequency	100kHz
D	Switching duty cycle	0.7
t_d	Estimated delay time	5uSec
R_L	Load resistance	450Ω

DC transfer functions of $H_{Vo-VI}(D)$ and $H_{Vo-D}(D)$ is traced using Matlab and shown in Figure 13 and 14, respectively. By considering (15) and (24), Bode plot of small signal transfer functions of audio success-ability and control-to-output are depicted in Figures 15, 16.
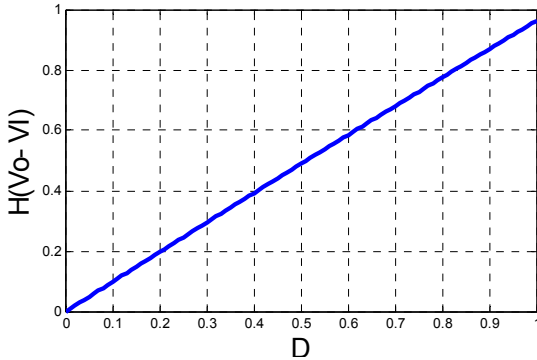
Fig. 13. DC transfer function of input-to-output voltage
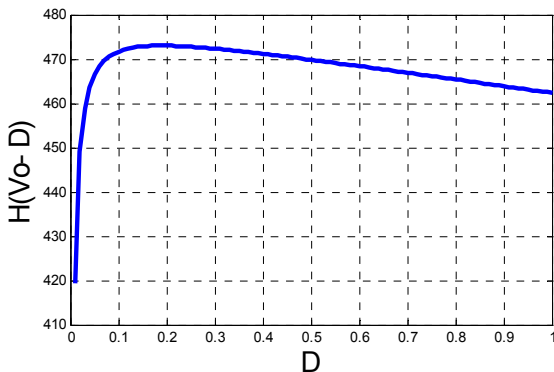
Fig. 14. DC transfer function of control-to-output voltage

Control to output transfer function help designer to better tune the control loop. As in Fig. 16, it is perceived that the operating point of the converter is not suitable for duty ratio lower 10% because the gain margin will be near zero.
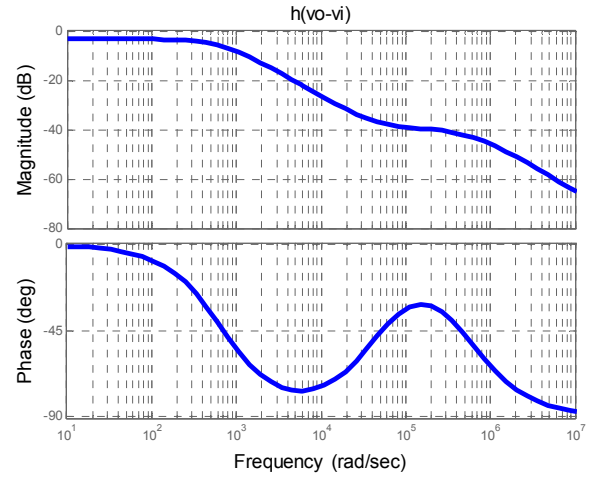
Fig. 15. Small signal transfer function of audio success-ability
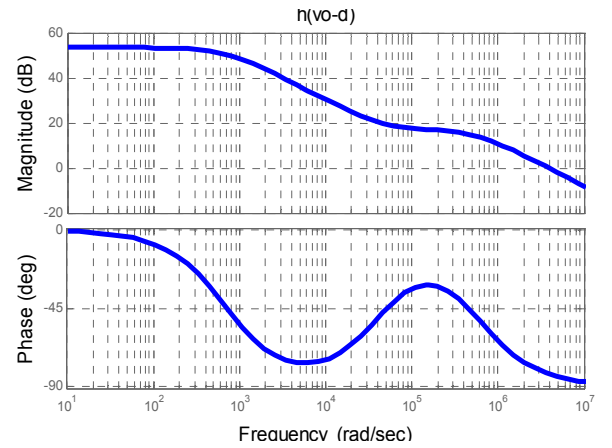
Fig. 16. Small signal transfer function of control-to-output

An external resistor is serried with capacitor ESR, first to protect the diode bridge from starting surge current because initial voltage of capacitor is zero and second to increase the zero frequency of small signal transfer function, The transfer function of the plant is also called the control-to-output transfer function; It is the output voltage of the converter, divided by the control voltage. As mentioned before, small signal model results are valid up to half of switching frequency. For this case f'$_{s1}$ is equal to $2f_{s1}$, thus Figures 15 and 16's data are reliable between 0:50 kHz range. Phase margin of audio success-ability is +95° and for control-to-output case is 180° approximately.

According to Table 1, converter components value is selected such its dynamic response stays in the over damped regime (ξ>1). Since any over shoot of V'$_o$ may exceeds the transistor and diodes breakdown voltage and damages them. Figure 17, shows the MOSFET gate signals of T_1 and T_2. This Figure and consequent ones is traced using analogue LEADER type oscilloscope. Ringing due to leakage inductance's only adds to peak voltage stress. We want to minimize this stress by having maximum power.
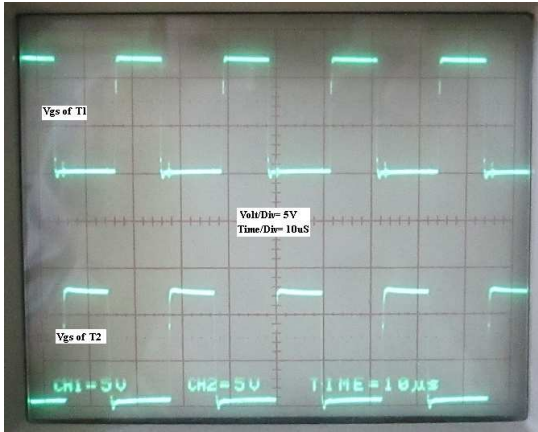
Fig. 17.T_1 and T_2 gate signals.

The transient component of the output voltage of inverter is given by Eq. (25), ΔV_I is a step change of input voltage.

$$v_o(s) = \frac{\Delta V_I}{s} \times h_{v_o - v_i}(s) \Rightarrow v_o(t) = \zeta^{-1}[v_o(s)] \quad (25)$$

Figures 18 and 19, show the step response of the transient component of the output voltage v'_o to a step change in the input voltage V_I from 12 to 12.7V which corresponds to a step change in small signal v_i from 0 to 0.7V for experimental and modelling cases respectively.
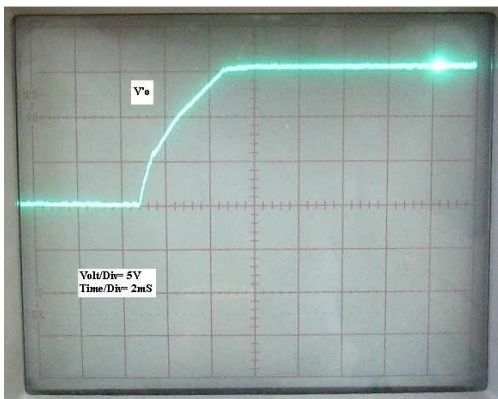
Fig. 18.v_o response to a change in v_i from 0 to 0.7V (Experiment)
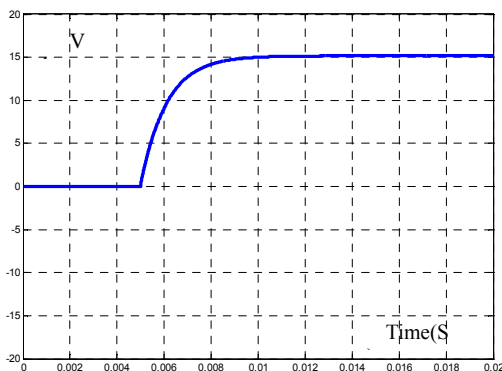
Fig. 19.v_o response to a change in v_i from 0 to 0.7V (Modelling)

Similarly to Eq. (26) can deduce the transient response of v_o to step change of the duty cycle as given by Eq. (26).

$$v_o(s) = \Delta d(s) \times h_{v_o - d}(s) \Rightarrow v_o(t) = \zeta^{-1}[v_o(s)] \quad (26)$$

To have variation, in this case duty cycle changes from 0.7 to 0.6 and endures 7ms on this state, then returns to its prior value that is stated and depicted in Eqs. (27), (28) and Figures 20, 21.

$$d(t) = D + k(u(t) - u(t - t_0));$$
$$where \ k = -0.1, \ t_0 = 7ms \quad (27)$$

$$\Delta d(s) = \frac{k}{s}(1 - e^{-st_0}) \quad (28)$$
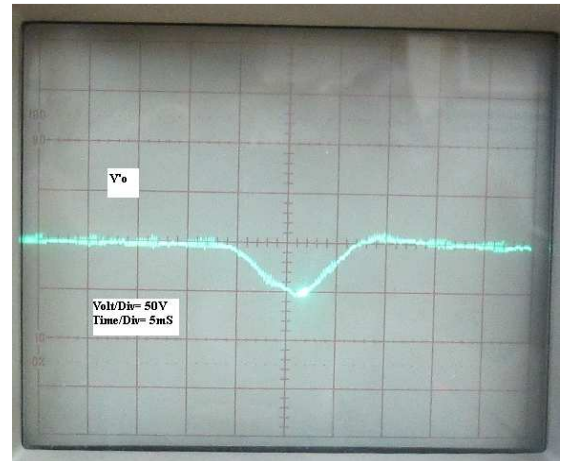
Fig. 20.v_o response to a temporary step change in d (Experiment)
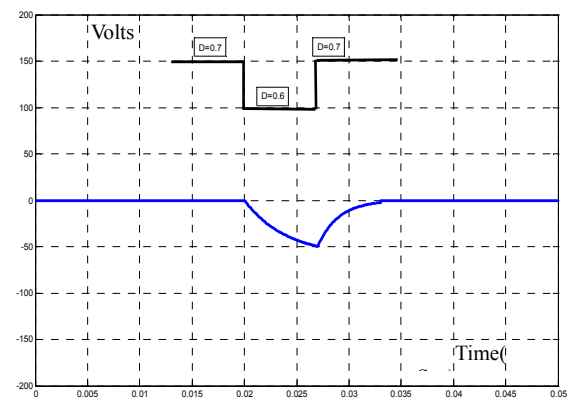
Fig. 21.v_o response to a temporary step change in d (Modelling)

It may be noted here that as long as inductor current is continuous the peak-to-peak ripple inthe inductor current is not affected by the dc value of load current. For constant outputvoltage and constant current through load, the inductor current ripple depends only on theduty ratio, which in turn depends on the input dc voltage.

6. Conclusion

This paper presents a methodology to get the dc and ac small signal transfer functions of audio success-ability and control-to-output of the converter. This method is based on averaged switch network modelling. The model developed here with the PWM switch modeling method can be implemented in any circuit oriented simulation tool. It is a nonlinear, large signal, averaged model. The nonlinearity due to the switching process in a converter and its parasitic elements is included in the model. Other nonlinearities, such as the duty ratio limitation, can easily be modeled. The same model can also be used for frequency domain simulations. The advantage of this modelling technique in comparison with usual state space averaging method is stated. Taking into account the parasitic elements is to better estimate the quiescent point and dynamic response of the converter. Finally, experimental test setup results for a given converter case indicate the validity and accuracy of the proposed modelling technique. The overall modelling error was under 3%, and the comparative study proves a good match between modelling and experimental results.

References

[1] B.J. Patella, A. Prodic, A. Zirger and D. Maksimovic, "High-frequency digital PWM controller IC for DC-DC converters,"*IEEE Trans. Power Electronics*, Vol.18,No.1, p.438-446, Jan. 2003.

[2] R.J. Wai, L.C. You and R.Y. Duan, "High efficiency DC/DC converter with voltage gain power applications,"*IEEE Trans. IndustrialElectronics*, Vol.54, No.1, p.354-364,Mar.2007.

[3] S.H.Tu and C.T. Lee, "A PWM Controller with Multiple-Access Table Look-up for DC-DC Buck Conversion,"*International Journal of Electronics and Engineering*, Vol. 3, No. 6, pp. 1321-1324, 2009.

[4] D.C. Hamill, J. H. B. Deane and D. J. Jefferies, "Modelling of chaotic DC-DC converters by iterated nonlinear mappings,"*IEEE Trans. Power Electronics*,Vol. 7, No. 1, pp. 25-36, Jan 1992.

[5] P. Klimczak and S.M. Nilsen, "Comparative study on paralleled vs. scaled DC-DC converters in high voltage gain applications,"*Power electronic and Motion Control Conference*,Vol. 1, pp. 18-13, 2008.

[6] H.R.E. Larico, D.S. Greff and J.A. Heerdt, "Modelling and control of a three-phase push-pull dc-dc converter: Theory and simulation,"*IEEE Brazilian Power Electronics Conference,* pp. 1-5, 2015.

[7] J.H. Deane and D Hamil, "Improvement of power supply EMC by chaos,"*Electronics Letters*, Vol. 32, No. 12, pp. 1045-1048, Jul. 1996.

[8] G. Zhang, Y. Liao, S.S. Yu and Y. Zhang, "A Graph-Modelling Approach to Topology Simplification in Power Converters,"*IEEE Trans. Power Electronics*,Vol. 37, No. 7, pp. 8248-8261, Jul. 2022.

[9] M. Kaya, A. Costabeber, A.J. Watson, F. Tardelli and J.C. Clare, "A Push-Pull Series Connected Modular Multilevel Converter for HVdc Applications,"*IEEE Trans. Power Electronics*, Vol. 37, No. 3, pp. 3111-3129, Mar. 2022.

[10] A. Aldana, O. Beltran and C. Rodrigez, "Design Modelling and Implementation of a Push-Pull Converter used in Grid Connected Photovoltaic Systems,"*Journal of Engineering Science and Technology Review*, Vol. 11, No. 4, pp. 132-137, 218.

[11] M.L. Flach, L.G. Scherer and R.F. Camargo, "Development of a Hybrid Microgrid for Power Generation through the Interconnection of Sources with a Push-Pull Converter,"*2021 Brazilian Power Electronics Conference (COBEP)*, pp. 1-8, 2021.

[12] U.S.Padiyar and R. Kalpana, "Design & Analysis of Push-pull Converter Fed Battery Charger for Electric Vehicle Application,"*IEEE International Conference on Power Electronics Smart Grid and Renewable Energy (PESGRE)*, pp. 1-6, Jun. 2022.

[13] S. Lim, J. Ranson, D.M. Otten and D.J. Perreault, "Two-Stage Power Conversion Architecture Suitable for Wide Input Voltage,"*IEEE Trans. Power Electronics*, Vol. 30, No. 2, pp. 805-816, Feb. 2015.

[14] C. Fei, M.H. Ahmed, F.C. Lee and Q. Li, "Dynamic bus voltage control for light load efficiency improvement of two-stage voltage regulator,"*IEEE Energy Conversion Congress and Exposition (ECCE)*, pp. 1-8, 2016.

[15] I. Barbi and R. Gules, "Isolated DC-DC converters with high-output voltage for TWTA tele-communication applications,"*IEEE Trans. Power Electronics*,Vol. 18, No. 4, pp. 975-984, Jul. 2003.

[16] A. Ferreres, J.A. Carrasco, E. Maset and J.B. Ejea, "Small-signal modelling of a controlled transformer parallel regulator as a multiple output converter high efficient post-regulator,"*IEEE Trans. Power Electronics*,Vol. 19, No. 1, pp. 183-191, Jan. 2004.